Diagnosis of Stator High Resistance Connection Based on Multiple Reference Frame Controllers in Asymmetrical Six-Phase AC PMSM Drives

Published Version:
Gritli, Y., Rossi, C., Mengoni, M., Tani, A., Casadei, D. (2025). Diagnosis of Stator High Resistance Connection Based on Multiple Reference Frame Controllers in Asymmetrical Six-Phase AC PMSM Drives. NEW YORK : Institute of Electrical and Electronics Engineers Inc. [10.1109/ONCON62778.2024.10931276].

Availability:
This version is available at: https://hdl.handle.net/11585/1013681 since: 2026-07-08

Published:
DOI: http://doi.org/10.1109/ONCON62778.2024.10931276

(Article begins on next page)

Diagnosis of Stator High Resistance Connection Based on Multiple Reference Frame Controllers in Asymmetrical Six-Phase AC PMSM Drives

Yasser Gritli
Dept. of Electrical, Electronic and Information Engineering "G. Marconi"
University of Bologna
Bologna, Italy
yasser.gritli@unibo.it

Claudio Rossi
Dept. of Electrical, Electronic and Information Engineering "G. Marconi"
University of Bologna
Bologna, Italy
claudio.rossi@unibo.it

Michele Mengoni
Dept. of Electrical, Electronic and Information Engineering "G. Marconi"
University of Bologna
Bologna, Italy
michele.mengoni@unibo.it

Angelo Tani
Dept. of Electrical, Electronic and Information Engineering "G. Marconi"
University of Bologna
Bologna, Italy
angelo.tani@unibo.it

Domenico Casadei
Dept. of Electrical, Electronic and Information Engineering "G. Marconi"
University of Bologna
Bologna, Italy
domenico.casadei@unibo.it

***Abstract*— Increasing interest has been shown in multiphase drives for medium and high-power industrial applications, owing to their specific advantages when compared to their three-phase counterparts. High-resistance connections cause stator resistance unbalance, leading to a degraded performance of the machine, which in turn affects the efficiency and reliability of the machine and the overall system.**

In this paper, an improved field-oriented control scheme is designed to detect stator high-resistance connections, localize the affected phase/phases, and compensate the effect of the stator fault in order to keep the drive behavior nearly unchanged until a safe procedure to stop the drive is activated. The proposed control strategy is based on an analytical model that takes into account the stator resistance unbalance introduced by a high resistance connection, exploiting the control signals derived from multi-reference frame current regulators.

The theoretical analysis of the diagnosis approach and the corresponding fault-tolerant control strategy are fully tested by numerical simulations.

Keywords*— *Fault diagnosis, high resistance connection, electrical fault detection, fault location, fault tolerance, permanent magnet motors, variable speed drive.

I. INTRODUCTION

Multiphase machines have gained significant interest by the research community in the last decade, becoming a feasible solution for a wide range of industrial applications. Actually, multiphase Permanent Magnet Synchronous Motors (m-PMSMs) are well recognized as a favored choice for applications requiring high reliability, ranging from traction systems to energy generation systems [1], [2]. Due to their high-power density, large power-to-weight ratio, high efficiency, and high torque-to-current ratio, m-PMSM represent a potential solution for modern aerospace or traction systems, as well as several applications requiring high availability and fault tolerance capabilities [2], [3].

However, m-PMSM are exposed to stator faults which, if not detected and localized at incipient stage, can propagate leading to serious damages for the whole drive [4].

High-resistance connections (HRCs) are common problems that can affect the stator winding connections at the motor terminals and/or the power devices connected between the machine and the supply source in industrial drives [5], [6]. They are generally caused by a combination of poor workmanship, thermo-mechanical effects, and/or contact surface damage. Thus, the contact resistance increase is accelerated, leading to localized thermal overloading, which imposes a voltage unbalance to the motor. It can be concluded that the propagation of HRC will not only affect the concerned stator phases, but also the mechanical parts and very probably shortening its lifetime.

The classical techniques for detecting HRC include the offline resistive imbalance test, or visual inspection. Reliable sensorless techniques dedicated to online monitoring, which are based on negative-sequence current and zero-sequence voltage have been proposed for three-phase machines [7], [8]. Different techniques for the diagnosis of stator faults have been developed. Impressive research efforts have been carried out in recent years for the development of fault-tolerant strategies under faults for m-PMSMs [9], [10], [11], [12]. In [12], two current control modes, that tolerate an open-phase fault for six-phase PMSM, which provide minimum stator losses and maximum torque output are developed.

An attractive approach based on the combination of merits of both common and separate neutral point configurations for optimizing the performances under open-phase fault for six-phase PMSM, is presented in [10]. A postfault decoupling model with reduced-order transformation is established for six-phase PMSM in [13], where the current references are reconfigured with the aim to ensure minimum losses and torque maximization. An interesting diagnosis technique developed for five-phase PMSM is developed in [14]. The proposed approach is based on the combined use of the so-called "magnetic field pendulous oscillation" and the

This work was supported in part by the Italian MUR for financial support through MOST - Sustainable Mobility Center, Centro Nazionale per la Mobilita` Sostenibile, Spoke 13 of the National Recovery and Resilience Plan (PNRR). Mission 4, component 2, investment 1.4 e D.D. 1033 17/06/2022, CN00000023.

symmetrical components method. Although the experimental effectiveness of the proposed approach, for detecting and localizing the fault, the necessity of operating at steady state condition remains its main limitation.

In [15], the model of a five-phase PMSM, under mixed stator HRC, and rotor demagnetization, was developed. An IFOC scheme that can maintain a nearly undisturbed behavior of the system, and furthermore detect and localize stator HRC is presented. Recently, the control principle developed in [15] was extended to six-phase PMSM, and experimentally validated in [16], where the detection process of HRC was based on tracking the output voltage of a current regulator implemented on the plane d_5-q_5, dedicated to the compensation of the inverse component introduced by the stator HRC.

The main contribution of this paper is the fact that the assessment of the developed model under HRC exploits all the available subspaces to develop the principle of the fault tolerant control, and to design an on-line quantitative detection and localization methodology for six-phase PMSMs. More specifically, here the proposed strategy for on-line quantitative fault-detection and fault-localization is based on the exploitation of all the additional current regulators implemented to neutralize the disturbances imposed by the HRC on the stator currents. The theoretical analysis of the proposed strategy for online quantitative fault-detection and fault-localization associated to the fault-tolerant control scheme are analytically developed and tested by numerical simulations.

II. Six-Phase PMSM Modeling

The motor considered is a 30° asymmetrical six-phase PMSM affected by HRC, with separated neutral points (Fig. 1). The developed model is valid in the general case of six different stator resistances.

Based on the concept of the Vector Space Decomposition (VSD) principle [16], [17], and the stator winding design with two isolated neutral points, leading to stator current in the 3rd subspace equal to zero, the formulation of the voltage equations, expressed in the stator reference frame, can be limited to the 1st and 5th subspaces as:

$$\bar{v}_{S1} = R_{S0}^{+}\,\bar{i}_{S1} + \bar{R}_{S10}^{*}\,\bar{i}_{S1}^{\,*} + \bar{R}_{S4}^{*}\,\bar{i}_{S5} + R_{S0}^{-}\,\bar{i}_{S5}^{*} + \frac{d\bar{\varphi}_{S1}}{dt} \qquad (1)$$

$$\bar{v}_{S5} = \bar{R}_{S4}\,\bar{i}_{S1} + R_{S0}^{-}\,\bar{i}_{S1}^{\,*} + R_{S0}^{+}\,\bar{i}_{S5} + \bar{R}_{S10}\,\bar{i}_{S5}^{*} + \frac{d\bar{\varphi}_{S5}}{dt} \qquad (2)$$

The upper symbol "*" is used to represent the complex conjugate value of a variable. As can be evidenced in (1) and (2), the stator resistance voltage drops are described by two real (R_{S0}^{+}, R_{S0}^{-}) and two complex ($\bar{R}_{S10}, \bar{R}_{S4}$) resistance components, which are defined by the following transformations:

$$R_{S0}^{+} = \frac{1}{6}\left[R_{Sa1} + R_{Sa2} + R_{Sb1} + R_{Sb2} + R_{Sc1} + R_{Sc2}\right] \qquad (3)$$

$$R_{S0}^{-} = \frac{1}{6}\left[R_{Sa1} - R_{Sa2} + R_{Sb1} - R_{Sb2} + R_{Sc1} - R_{Sc2}\right] \qquad (4)$$

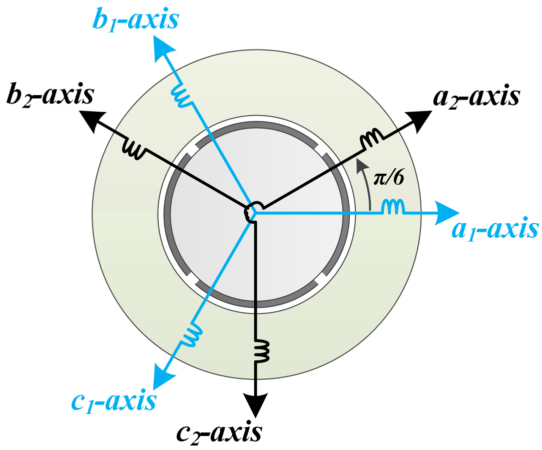

Fig. 1. Asymmetrical six-phase surface-mounted PMSM with two separated neutral points.

$$\bar{R}_{S4} = \frac{1}{6}\Big[R_{Sa1} + R_{Sa2}\bar{\alpha}^{4} + R_{Sb1}\,\bar{\alpha}^{4} + R_{Sb2}\,\bar{\alpha}^{8} + R_{Sc1}\,\bar{\alpha}^{8} + R_{Sc2}\Big] \qquad (5)$$

$$\bar{R}_{S10} = \frac{1}{6}\Big[R_{Sa1} + R_{Sa2}\bar{\alpha}^{10} + R_{Sb1}\,\bar{\alpha}^{4} + R_{Sb2}\,\bar{\alpha}^{2} + R_{Sc1}\,\bar{\alpha}^{8} + R_{Sc2}\,\bar{\alpha}^{6}\Big] \qquad (6)$$

where $\bar{\alpha} = e^{j\pi/6}$.

The stator flux space vectors can be formulated as

$$\bar{\varphi}_{S1} = L_{S1}\,\bar{i}_{S1} + 2\,\varphi_{M1}\cos(\gamma)\,e^{j\theta} + 2\,\varphi_{M11}\cos(11\,\gamma)\,e^{-j11\theta} \qquad (7)$$

$$\bar{\varphi}_{S5} = L_{S5}\,\bar{i}_{S5} + 2\,\varphi_{M5}\cos(5\,\gamma)\,e^{j5\theta} + 2\,\varphi_{M7}\cos(7\,\gamma)\,e^{-j7\theta} \qquad (8)$$

where $\gamma = (\pi - \beta)/2$ and β is the magnet pole arc in electrical radians.

Based on the previous formulations, the electromagnetic torque T_{em} can be formulated as

$$\begin{aligned} T_{em} = {} & 6\,p\,\phi_{M1}\left[\bar{i}_{S1}\cdot j\,\cos(\gamma)\,e^{j\theta}\right] \\ & + 30\,p\,\phi_{M5}\left[\bar{i}_{S5}\cdot j\,\cos(5\,\gamma)\,e^{j5\theta}\right] \\ & + 42\,p\,\phi_{M7}\left[\bar{i}_{S5}^{*}\cdot j\,\cos(7\,\gamma)\,e^{j7\theta}\right] \\ & + 66\,p\,\phi_{M11}\left[\bar{i}_{S1}^{*}\cdot j\,\cos(11\,\gamma)\,e^{j11\theta}\right] \end{aligned} \qquad (9)$$

where the constant values $\phi_{M\rho}$ depend on the rotor permanent magnet shape and the stator winding arrangement.

Based on the torque expression (9), and besides the fundamental component, different additional oscillating contributions can be evidenced. Thus, in order to ensure a uniform torque, the control system should be tuned for keeping $\bar{i}_{S5}$ equal to zero. Whereas a specific machine design can be adopted for minimizing the contribution of the 11th flux harmonic, which was practically achieved by using a stator winding pitch of 165°.

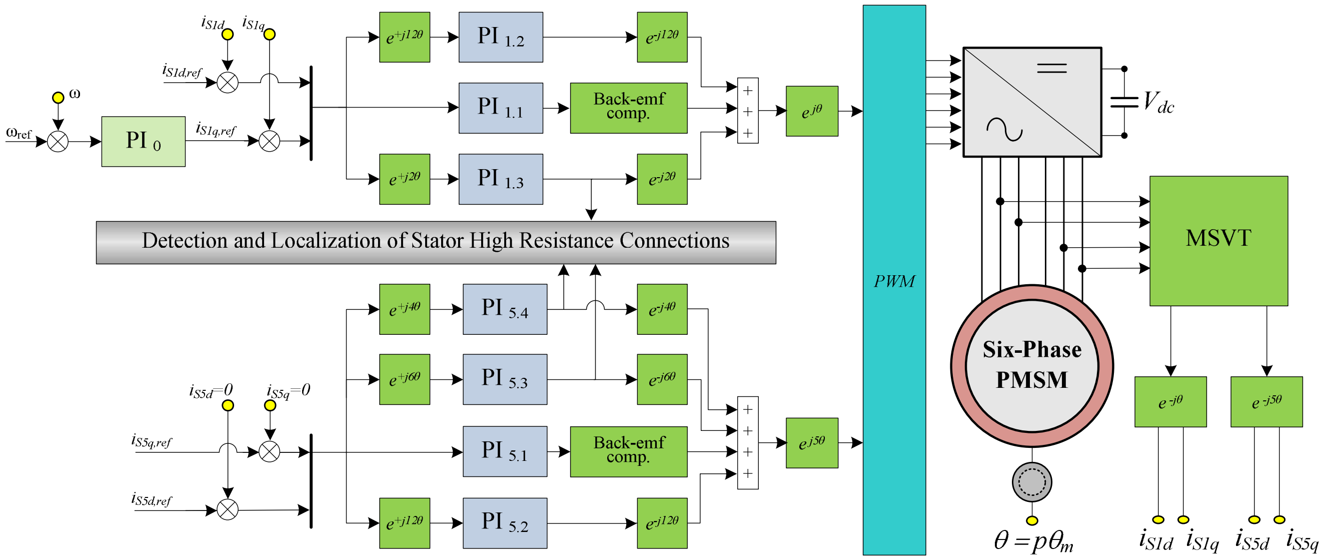

Fig. 2. Block diagram of the proposed control scheme.

III. HRC Fault Tolerant Control

To better emphasize the principle of the proposed IFOC strategy, it is useful to reformulate the stator voltage equations (1)-(2) in the rotating reference frames, where the needed current regulators are conventionally implemented. Substituting the stator flux space vectors formulated by (7)-(8) into (1)-(2), respectively, and applying the adequate transformations from stator to rotating reference frames (superscript “r”), the new stator voltage equations can be written as

$$\bar{v}_{S1}^{r} = R_{S0}^{+}\,\bar{i}_{S1}^{r} + \bar{v}_{S1,HRC}^{r} + L_{S1}\frac{d\bar{i}_{S1}^{r}}{dt} + j\omega L_{S1}\,\bar{i}_{S1}^{r} + j2\omega\,\phi_{M1}\cos(\gamma) - j22\omega\,\phi_{M11}\cos(11\,\gamma)\,e^{-j12\theta} \quad (10)$$

$$\bar{v}_{S5}^{r} = \bar{v}_{S5,HRC}^{r} + j10\omega\,\phi_{M5}\cos(5\,\gamma) - j14\omega\,\phi_{M7}\cos(7\,\gamma)\,e^{-j12\theta} \quad (11)$$

where

$$\bar{v}_{S1,HRC}^{r} = \bar{R}_{S10}^{*}\,\bar{i}_{S1}^{r*}\,e^{-j2\theta} \quad (12)$$

$$\bar{v}_{S5,HRC}^{r} = \bar{R}_{S4}\,\bar{i}_{S1}^{r}\,e^{-j4\theta} + R_{S0}^{-}\,\bar{i}_{S1}^{r*}\,e^{-j6\theta} \quad (13)$$

It is worth noting that the space vectors $\bar{v}_{S1,HRC}^{r}$ and $\bar{v}_{S5,HRC}^{r}$ represent the voltage drops introduced by the stator HRC, in the d_1-q_1 and d_5-q_5 planes, respectively.

The basic FOC strategy is often adopted for multiphase PMSM, where the control scheme for six-phase configuration can be clearly identified by the current controllers $PI_{1.1}$, $PI_{5.1}$, $PI_{1.2}$ and $PI_{5.2}$ illustrated in Fig. 2. The basic FOC configuration can be improved in such a manner that the performances of the machine are not altered by stator HRC. Examining the formulation of the stator voltages (10)-(11), the quantities $\bar{v}_{S1,HRC}^{r}$ and $\bar{v}_{S5,HRC}^{r}$ appear as disturbing quantities caused by the presence of HRC. In order to cope with these disturbing effects, an Improved FOC (IFOC) is proposed (Fig. 2). For correct stator current reference tracking, three additional current controllers, namely $PI_{1.3}$, $PI_{5.3}$ and $PI_{5.4}$, have been implemented in reference frames synchronized with the different angular speeds of the voltage vectors drops $\bar{v}_{S1,HRC}^{r}$ and $\bar{v}_{S5,HRC}^{r}$.

Finally, it is important to note that the output voltages of the added current controllers $PI_{1.3}$, $PI_{5.3}$ and $PI_{5.4}$, can be very useful for implementing the new on-line stator HRC diagnosis strategy suitable for six-phase PMSM drives. This issue will be investigated in the next section.

IV. HRC Fault Detection and Localization

Based on the voltage space vectors (10)-(13), expressed in the rotating reference frames, the proposed IFOC scheme is able to achieve a proper tracking of the reference stator current space vectors $\bar{i}_{S1,ref}^{r}$ and $\bar{i}_{S5,ref}^{r} = 0$, in healthy conditions as well as under stator HRC.

Examining the four stator resistance components expressed in (3)-(6), one can note that under balanced stator resistance for the healthy case, only R_{S0}^{+}, i.e. the mean value of the six stator resistances, is different from zero. Thus, the remaining three components R_{S0}^{-}, $\bar{R}_{S4}$, $\bar{R}_{S10}$ are representative of the stator HRC that can affect the symmetry of the six phase-resistances.

According to (10)-(13), and taking into account the behavior of the proposed IFOC control scheme (Fig. 2), it is possible to recognize that the voltage outputs of the current controllers $PI_{1.3}$, $PI_{5.3}$ and $PI_{5.4}$ assume the following expressions

$$\bar{v}_{PI1.3} = \bar{R}_{S10}^{*}\,\bar{i}_{S1}^{r*} \quad (14)$$

$$\bar{v}_{PI5.3} = R_{S0}^{-}\,\bar{i}_{S1}^{r*} \quad (15)$$

$$\bar{v}_{PI5.4} = \bar{R}_{S4}\,\bar{i}_{S1}^{r} \quad (16)$$

According to (14)-(16), the estimated stator resistance components R_{S0}^{-}, $\bar{R}_{S4}$, $\bar{R}_{S10}$ can be estimated as

$$\hat{R}^{-}_{S0} = \frac{\bar{v}_{PI\,5.3}}{\bar{i}^{r*}_{S1}} \tag{17}$$

$$\hat{\bar{R}}_{S4} = \frac{\bar{v}_{PI\,5.4}}{\bar{i}^{r}_{S1}} \tag{18}$$

$$\hat{\bar{R}}^{*}_{S10} = \frac{\bar{v}_{PI\,1.3}}{\bar{i}^{r*}_{S1}} \tag{19}$$

Based on the inverse transformations, corresponding to those formulated by (3)-(6), and taking into account the estimated stator resistance components expressed in (17)-(19), the estimated phase resistance deviations with respect to their mean value can be evaluated by the following equations

$$\Delta\hat{R}_{Sa1} = \hat{R}^{-}_{S0} + \hat{\bar{R}}_{S4} + \hat{\bar{R}}_{S4}{}^{*} + \hat{\bar{R}}_{S10} + \hat{\bar{R}}_{S10}{}^{*} \tag{20}$$

$$\Delta\hat{R}_{Sa2} = -R^{-}_{S0} + \bar{R}_{S4}\bar{\alpha}^{8} + \bar{R}_{S4}{}^{*}\bar{\alpha}^{4} + \bar{R}_{S10}\bar{\alpha}^{2} + \bar{R}_{S10}{}^{*}\bar{\alpha}^{10} \tag{21}$$

$$\Delta\hat{R}_{Sb1} = \hat{R}^{-}_{S0} + \hat{\bar{R}}_{S4}\bar{\alpha}^{8} + \hat{\bar{R}}_{S4}{}^{*}\bar{\alpha}^{4} + \hat{\bar{R}}_{S10}\bar{\alpha}^{8} + \hat{\bar{R}}_{S10}{}^{*}\bar{\alpha}^{4} \tag{22}$$

$$\Delta\hat{R}_{Sb2} = -R^{-}_{S0} + \bar{R}_{S4}\bar{\alpha}^{4} + \bar{R}_{S4}{}^{*}\bar{\alpha}^{8} + \bar{R}_{S10}\bar{\alpha}^{10} + \bar{R}_{S10}{}^{*}\bar{\alpha}^{2} \tag{23}$$

$$\Delta\hat{R}_{Sc1} = \hat{R}^{-}_{S0} + \hat{\bar{R}}_{S4}\bar{\alpha}^{4} + \hat{\bar{R}}_{S4}{}^{*}\bar{\alpha}^{8} + \hat{\bar{R}}_{S10}\bar{\alpha}^{4} + \hat{\bar{R}}_{S10}{}^{*}\bar{\alpha}^{8} \tag{24}$$

$$\Delta\hat{R}_{Sc2} = -R^{-}_{S0} + \bar{R}_{S4} + \bar{R}_{S4}{}^{*} + \bar{R}_{S10}\bar{\alpha}^{6} + \bar{R}_{S10}{}^{*}\bar{\alpha}^{6} \tag{25}$$

By monitoring the values of the six resistance variations (20)-(25) it is possible to ensure a clear detection and localize the extend of the HRC propagation.

V. SIMULATION RESULTS

To evaluate the performance of the proposed IFOC architecture and the associated diagnosis strategy (Fig. 2), the controlled six-phase PMSM drive was implemented in Matlab/Simulink™ for numerical simulations. The main parameters of the motor are listed in Table I, which corresponds to the real machine used for the experimental tests. HRC fault was emulated by additional resistors in series with the phase affected by the fault. Initially, the six-phase PMSM was controlled by the basic FOC algorithm configuration, where only the current regulators $PI_{1.1}$, $PI_{1.2}$, $PI_{5.1}$, and $PI_{5.2}$ are activated. The simulations were carried out under healthy and HRC fault (Radd=1.0 p.u.) in phase a1.

The corresponding current waveforms of phases a1 and b2 are reported in Fig. 3-a and Fig. 3-b, respectively, where the current magnitude variation from healthy to faulty conditions can be observed. A third simulation was carried out, where the six-phase PMSM is unbalanced by the phase a1 (Radd=1.0 p.u.) but controlled by the proposed IFOC algorithm. As can be seen in Fig. 3-c, the machine operation is regular with balanced currents (Fig. 3-c), confirmed by a null current space vector of $\bar{i}_{S5}$ on plane α_5-β_5 (Fig. 3-f), leading to a good ability of the proposed IFOC to compensate the effects of unbalance although the important degree of unbalance with 1.0 p.u. of R_s in phase a1.

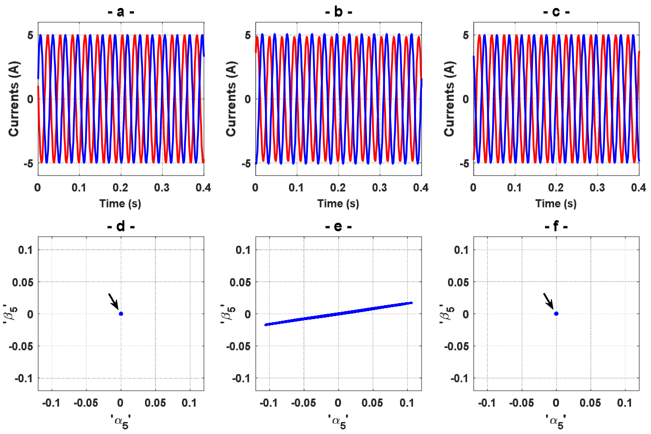

Fig. 3. Behavior of the drive when the six-phase PMSM operates at rated speed and 50% of the rated load. (a) Healthy machine controlled by a standard FOC. Unbalanced machine by phase a1 (Radd=1.0 p.u.) when controlled by (b) a standard FOC, and (c) the proposed IFOC. (d)-(f) Loci of the current space vector on plane α_5-β_5 corresponding to the (a)-(c) conditions, respectively.

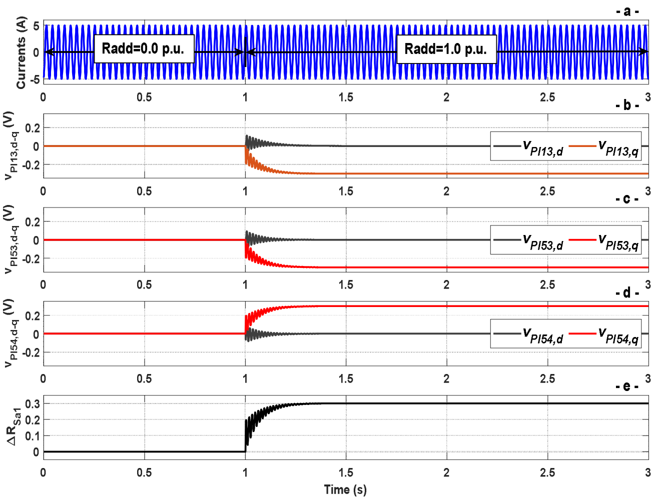

Fig. 4. Simulation results: Behavior of the drive when the six-phase PMSM is controlled by the IFOC and is operated at 1000 r/min with 50% of the rated load. (a) Stator current of phase a1. Waveforms of the d-q voltage outputs of the current controller (b) $PI_{1.3}$, (c) $PI_{5.3}$, and (d) $PI_{5.4}$. (e) Estimated resistance variation of the stator phase a1 with respect to the actual average value.

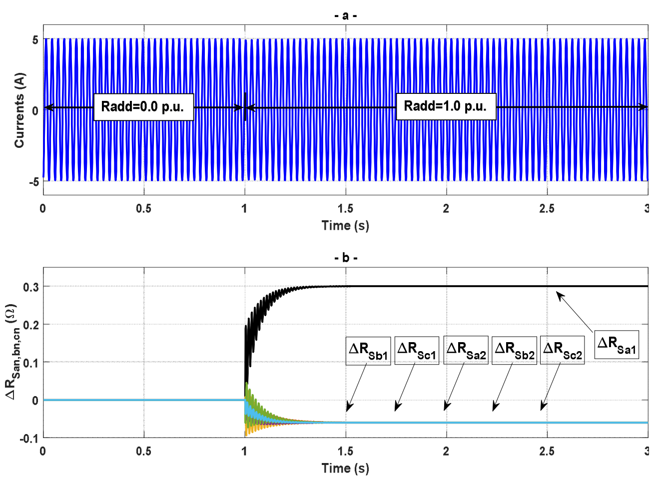

Fig. 5. Simulation results: Behavior of the drive when the resistance of phase a1 is increased by 0.36 Ω. The six-phase PMSM is controlled by the IFOC and is operated at 1000 r/min with 50% of the rated load. (a) Stator current of phase a1. (b) Resistance variations of the stator phases with respect to the actual average value.

TABLE I. PARAMETERS OF SIX-PHASE PMSM

Phase resistance	0.36	Ohm
Pole number	4	-
Phase inductance	1.44	mH
Slot number	48	-
Stator winding pitch	165°	el. degrees
Rated speed	1000	rpm

In Fig. 4, the behavior of the proposed IFOC strategy, where the additional resistor (Radd) inserted in series to phase a1 is increased from zero to 1.0 p.u., is reported. Initially, the machine operates in healthy condition (Radd=0.0 Ω) during the first-time interval of 1 s. The d-q voltage components generated by the current controllers $PI_{1.3}$, $PI_{5.3}$, $PI_{5.4}$, and the resistance deviation ΔR_{Sa1} are equal to zero. As soon as the stator resistance R_{Sa1} increases of 1.0 p.u. (0.36 Ω as rated value) at t=1s, the voltage components $v_{PI1.3,d-q}$, $v_{PI5.3,d-q}$, and $v_{PI5.4,d-q}$ change to compensate the effect of the stator asymmetry, and at the same instant (at t=1s) the resistance deviation ΔR_{Sa1} change from 0.0 Ω to about 0.3 Ω with respect to the average value of the phase resistances.

Theoretically, the mean value of the six phase resistances becomes 0.42 Ω. Thus, the expected resistance deviation ΔR_{Sa1} is 0.72-0.42 ≅ 0.3 Ω, which is validated by the numerical simulations result reported in Fig. 4-e, leading to an accurate full stator HRC detection and quantification.

In order to assess the ability of the proposed approach in terms of stator HRC localization, the resistance variations $\Delta R_{San,bn,cn}$ (n=1,2) of all phases have been evaluated and reported in Fig. 5, under the same operating conditions. As can be seen in Fig. 5-b, the resistance deviation ΔR_{Sa1} is of 0.3 Ω, whereas the remaining five deviations are respectively equal to 0.36-0.42 ≅ -0.06 Ω, leading to an accurate detection, quantification and localization of the stator fault.

Fig. 6 shows the behavior of the machine under two stator phases affected by HRC. Initially, the machine operates under healthy condition for a first-time interval of 1 s. Then, the resistances of phase a1 and b2 are incremented by 0.36 Ω and 0.18 Ω, respectively. The detailed behavior of the resistance deviations of all phases is reported in Fig. 6-b. With the actual mean value of the phase resistances (0.45 Ω), the resistance deviations of ΔR_{Sa1} and ΔR_{Sb2} are equal to 0.27 Ω and 0.09 Ω, respectively, whereas the remaining phase deviations are equal to -0.09 Ω. These theoretical values are clearly validated by simulation results reported in Fig. 6-b, leading to an effective quantitative detection and localization of the stator phases affected by HRC.

Finally, in order to evaluate the sensitivity of the proposed approach for detecting and localizing a phase affected by HRC, the PMSM was run at 1000 r/min with 50% of the rated load, for different stator HRC severities, i.e., Radd=0.18 Ω, 0.36 Ω (equal to Rs), 0.54 Ω, 0.72 Ω, 0.9 Ω, and 1.08 Ω, affecting phase-a1.

The behavior of each phase resistance variation, under the considered stator HRC severity cases, are reported in Fig. 7. Observing the proportional evolution of the resistance variation of phase a1, corresponding to the increments of unbalance, it is evident that the detection process adopted provide not only clear discrimination between healthy and

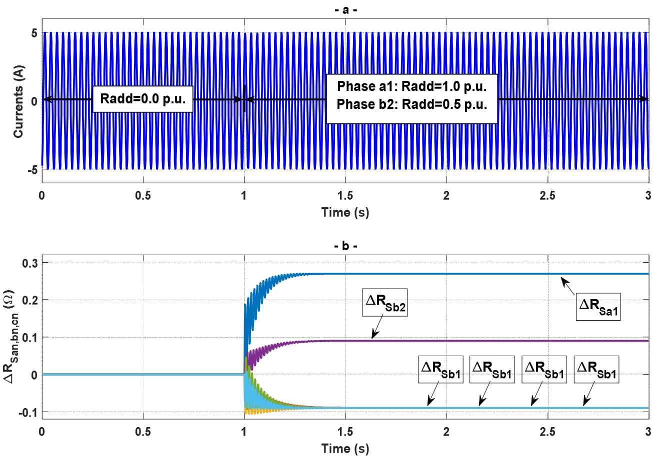

Fig. 6. Simulation results: Behavior of the drive when the resistances of phases a1 and b2 are increased by 0.36 Ω and 0.18 Ω, respectively. The six-phase PMSM is controlled by the IFOC and is operated at 1000 r/min with 50% of the rated load. (a) Stator current of phase a1. (b) Resistance variations of the stator phases with respect to the actual average value.

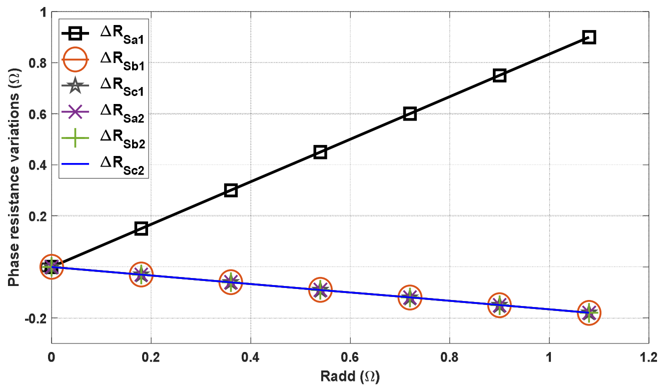

Fig. 7. Simulation results: Behavior of each phase resistance variation with respect to the average value, under different stator HRC severities affecting phase-a1. The six-phase PMSM is controlled by the IFOC and is operated at 1000 r/min with 50% of the rated load.

faulty conditions, but also an effective quantification of the HRC fault severity. Furthermore, the equal values of the phase resistance variation of the remaining five healthy phases, when compared to resistance variation of phase a1, confirms the ability of the proposed approach to localize the fault. It is worth noting that the more significant is the degree of HRC, the more the phase affected by the fault is quantitatively easier to be localized.

VI. CONCLUSION

The paper presents a new mathematical model for an asymmetrical six-phase PMSM under HRC fault, which exploits the additional degrees of freedom used to investigate the behavior of the motor in different α-β planes. The presented analytical model has a general validity, showing the possibility to investigate new diagnostic techniques based on monitoring the manipulated control signals in different reference frames. It is shown that the proposed strategy provides not only detection, but also effective localization of more than one phase affected by HRC fault.

Actually, the proposed strategy is experimentally implemented and have shown very promising results. A complete set of experimental tests under different conditions will be presented in a future publication.

REFERENCES

[1] E. Levi, "Multiphase electric machines for variable-speed applications," *IEEE Transactions on industrial electronics*, vol. 55, no. 5, pp. 1893–1909, 2008, doi: 10.1109/TIE.2008.918488.

[2] M. J. Duran, E. Levi, and F. Barrero, "Multiphase electric drives: Introduction," *in Encyclopedia of electrical and electronics engineering*, no. J. Webster, Ed. Hoboken, NJ, USA: Wiley, pp. 1–26, 2017, doi: 10.1002/047134608X.W8364.

[3] J. Xu, B. Zhang, H. Fang, and H. Guo, "Guaranteeing the fault transient performance of aerospace multiphase permanent magnet motor system: An adaptive robust speed control approach," *CES Transactions on Electrical Machines and Systems*, vol. 4, no. 2, pp. 114–122, 2020, doi: 10.30941/CESTEMS.2020.00016.

[4] S. Choi *et al.*, "Fault diagnosis techniques for permanent magnet ac machine and drives—A review of current state of the art," *IEEE Trans. Transp. Electrific.*, vol. 4, no. 2, pp. 444–463, 2018, doi: 10.1109/TTE.2018.2819627.

[5] J. Yun, J. Cho, S. Bin Lee, and J.-Y. Y. Yoo, "Online detection of high-resistance connections in the incoming electrical circuit for induction motors," *IEEE Trans Ind Appl*, vol. 45, no. 2, pp. 694–702, 2009, doi: 10.1109/TIA.2009.2013576.

[6] R. S. Colby, "Detection of high-resistance motor connections using symmetrical component analysis and neural network models," *IEEE-SDEMPED 2003*, no. August, pp. 2–6, 2003, doi: 10.1109/DEMPED.2003.1234538.

[7] J. Yun, J. Cho, S. B. Lee, and J. Yoo, "On-line detection of high-resistance connections in the incoming electrical circuit for induction machines," in *Proc. IEEE-IEMDC*, 2007, pp. 583–589. doi: 10.1109/TIA.2009.2013576.

[8] J. Yun, K. W. Lee, K. W. Lee, S. Bin Lee, and J. Y. Yoo, "Detection and classification of stator turn faults and high-resistance electrical connections for induction machines," *IEEE Trans Ind Appl*, vol. 45, no. 2, pp. 666–675, 2009, doi: 10.1109/TIA.2009.2013557.

[9] P. Gonçalves, S. Cruz, and A. Mendes, "Finite Control Set Model Predictive Control of Six-Phase Asymmetrical Machines—An Overview," *Energies (Basel)*, vol. 12, no. 24, p. 4693, 2019, doi: 10.3390/en12244693.

[10] H. M. Eldeeb, A. S. Abdel-Khalik, and C. M. Hackl, "Postfault full torque–speed exploitation of dual three-phase IPMSM drives," *IEEE Transactions on Industrial Electronics*, vol. 66, no. 9, pp. 6746–6756, 2019, doi: 10.1109/TIE.2018.2880698.

[11] Y. Gritli, M. Mengoni, G. Rizzoli, C. Rossi, A. Tani, and D. Casadei, "Rotor magnet demagnetisation diagnosis in asymmetrical six-phase surface-mounted AC PMSM drives," *IET Electr Power Appl*, vol. 14, no. 10, pp. 1747–1755, 2020, doi: 10.1049/iet-epa.2019.0222.

[12] Z. Changpan, T. Wei, Z. Zhaoji, Y. Guijie, and S. Jianyong, "Control strategy for dual three-phase PMSM based on reduced order mathematical model under fault condition due to open phases," *The Journal of Engineering*, vol. 2018, no. 13, pp. 489–494, 2018, doi: 10.1049/joe.2018.0061.

[13] Z. Liang, D. Liang, P. Kou, and S. Jia, "Postfault Control and Harmonic Current Suppression for a Symmetrical Dual Three-Phase SPMSM Drive Under Single-Phase Open-Circuit Fault," *IEEE Access*, vol. 8, pp. 67674–67686, 2020, doi: 10.1109/ACCESS.2020.2986790.

[14] H. Chen *et al.*, "High-Resistance Connection Diagnosis in Five-Phase PMSMs Based on the Method of Magnetic Field Pendulous Oscillation and Symmetrical Components," *IEEE Trans. Ind. Electron.*, vol. 69, no. 3, pp. 2288–2299, 2021, doi: 10.1109/TIE.2021.3065617.

[15] A. Tani *et al.*, "Detection of magnet demagnetization and high-resistance connections in five-phase surface-mounted permanent magnet generators," *Proceedings - SDEMPED 2015: IEEE 10th International Symposium on Diagnostics for Electrical Machines, Power Electronics and Drives*, pp. 487–493, 2015, doi: 10.1109/DEMPED.2015.7303734.

[16] C. Rossi, Y. Gritli, A. Pilati, G. Rizzoli, A. Tani, and D. Casadei, "High Resistance Fault-Detection and Fault-Tolerance for Asymmetrical Six-Phase Surface-Mounted AC Permanent Magnet Synchronous Motor Drives," *Energies (Basel)*, vol. 13, no. 12, p. 3089, 2020, doi: 10.3390/en13123089.

[17] G. Grandi, G. Serra, and A. Tani, "General analysis of multi-phase systems based on space vector approach," in *2006 12th International Power Electronics and Motion Control Conference*, IEEE, 2006, pp. 834–840. doi: 10.1109/EPEPEMC.2006.4778503.